A wide conserved DNA-damage-response-signaling cascade regulates proliferation *in planta* in the phytopathogenic fungus *Ustilago maydis*

Carmen de Sena-Tomas[1], Alfonso Fernández-Álvarez[2], William K. Holloman[3], and José Pérez-Martín[1*]

[1]Departamento de Biotecnología Microbiana, Centro Nacional de Biotecnología CSIC, Madrid, Spain

[2]Centro Andaluz de Biología del Desarrollo, Universidad Pablo de Olavide-CSIC, Sevilla, Spain

[3]Department of Microbiology and Immunology, Weill Cornell Medical College, New York, NY 10065 USA

*corresponding author

The author responsible for distribution of materials integral to the findings presented in this article in accordance with the policy described in the Instructions for Authors (www.plantcell.org) is Dr. José Pérez-Martín, Departamento de Biotecnología Microbiana, Centro Nacional de Biotecnología-CSIC, Campus de Cantoblanco-UAM, 28049 Madrid, Spain. Phone: +34-91-585-4704; FAX: +34-91-585-4506; e-mail: jperez@cnb.csic.es

Estimated Length of manuscript: 9.2 pages

Running title: Atr1-Chk1 and virulence in phytopathogenic fungi

ABSTRACT

In the phytopathogenic fungus *Ustilago maydis*, the dikaryotic state dominates the period of growth occurring during the infectious phase. Dikaryons are cells in which two nuclei, one from each parent cell, share a single cytoplasm for a period of time without undergoing nuclear fusion. In fungal cells, maintenance of the dikaryotic state requires an intricate cell division process that often involves the formation of a structure known as the clamp connection as well as the sorting of one of the nuclei to this structure to ensure that each daughter dikaryon inherits a balance of each parental genome. Here we describe an atypical role of the DNA-damage checkpoint kinases Chk1 and Atr1 during pathogenic growth of *U. maydis.* We found that Chk1 and Atr1 collaborate to control cell cycle arrest during the induction of the virulence program in *U. maydis*, and that Chk1 and Atr1 work together to control the dikaryon formation. These findings forge a new link between a widely conserved signaling cascade and the virulence program in a phytopathogen. We propose a model in which adjustment of the cell cycle by the Atr1-Chk1 axis controls fidelity in dikaryon formation. Therefore, Chk1 and Atr1 emerge as critical cell type regulators in addition to their roles in the DNA-damage response.

INTRODUCTION

The sexual life cycle starts with fusion of two different haploid cells, proceeds to the formation of a diploid, and ends with meiosis to generate four haploid cells (Chen et al., 2007). However the way in which haploid cells are brought together and the predominance of the haploid or diploid phase varies between species. In fungal cells, mating -the process equivalent to fertilization- brings together two haploid nuclei in the same cytoplasm. In some species of fungi this process is followed by nuclear fusion, resulting in a diploid nucleus that enters meiosis immediately (as occurs in the fission yeast *Schizosaccharomyces pombe*) or that is maintained and proliferates in the diploid state (as it happens in budding yeast *Saccharomyces cerevisiae*). However for a large group of fungi, mating results in a dikaryon, a cell in which the two nuclei -one from each parent cell- share a single cytoplasm for a period of time without undergoing nuclear fusion. The dikaryon represents an unusual cell type that often confers advantages in fitness over the monokaryotic counterparts (Clark and Anderson, 2004). The dikaryon stage is typical in the life cycles of many fungal species primarily in the Basidiomycota, a large group that includes mushrooms, bracket fungi and many phytopathogenic fungi, such as the corn pathogen *Ustilago maydis*.

Establishment and maintenance of dikaryotic growth in Basidiomycete fungi is controlled by information that is specified at the Mating Type (*MAT*) loci, specialized regions of fungal genomes akin to the sex chromosomes of larger eukaryotes (Lee et al., 2010). Although the specific contribution of the *MAT* locus components to dikaryon formation varies among species characterized

thus far, a central element common to all of them is the activation of a specific transcriptional cascade controlled by a heterodimeric homeodomain transcription factor, with components derived from the *MAT* locus of each parent. Dikaryotic maintenance involves an intricate cell division process to ensure that each dikaryon inherits a balance of each parental genome. In many dikaryotic basidiomycetes (with some exceptions such as various Uredinomycetes; for instance see (Ikeda et al., 2003) cell division involves the formation of a specialized structure known as the clamp connection, as well as the sorting of one of the nuclei to this structure. In this way nuclear division occurs in a synchronous and independent fashion in two distinct subcellular compartments. Once nuclear division is finished, the clamp connection is resolved to reconstitute the dikaryotic status of daughter cells (Brown and Casselton, 2001; Gladfelter and Berman, 2009). Studies with *Coprinopsis cinerea* and *Schizophyllum commune* indicated that the *MAT* genes encoding homeodomain transcription factors govern nuclear pairing as well as clamp formation (Casselton and Olesnicky, 1998; Kues, 2000), and therefore a connection between *MAT* genes and cell cycle control it is predicted, although the details behind these connections are largely unknown.

In *U. maydis*, the dikaryotic state dominates the period of growth occurring along the infectious phase. This state is dependent upon the *MAT*-encoded homeoprotein called b-complex, whose subunits -bW and bE- are provided by each mating partner (Feldbrugge et al., 2004; Brefort et al., 2009). During induction of the virulence program in *U. maydis*, an infectious dikaryotic hypha is produced on plant surface as a result of mating of a pair of compatible haploid budding cells. The infectious hypha or filament is composed of a

single dikaryotic cell that is arrested in the cell cycle at G2 phase (Mielnichuk et al., 2009), and its formation is dependent on synthesis of the b-complex. The arrest is transient and eventually the filament manages to enter the plant tissue, where it starts to proliferate while maintaining its dikaryotic status. Since mutations that abolishes this transient cell cycle arrest also impairs the dikaryon formation (Mielnichuk et al., 2009), it is thought that b-induced cell cycle arrest is required for dikaryon establishment in *U. maydis*. In our efforts to describe the mechanisms behind this transient cell cycle arrest, we recently reported that the widely conserved Chk1 protein kinase is required for this cell cycle arrest (Mielnichuk et al., 2009). Chk1 is better known as a key signal transducer within the DNA-damage response cascade (Chen and Sanchez, 2004) in a broad range of eukaryotes, including *U. maydis* (Perez-Martin, 2009). Here, we investigated the response of Chk1 to b-complex formation. We present findings showing that Chk1 is activated through phosphorylation by the conserved upstream activating kinase Atr1, and that the Atr1-Chk1 regulatory axis serves in maintenance of dikaryotic status *in planta*. Because Chk1 controls cell cycle progression, we propose that b-complex-mediated activation of Atr1-Chk1 axis is part of the mechanism responsible of coordination during a dikaryotic cell cycle.

RESULTS

b-dependent cell cycle arrest requires Chk1 activating phosphorylation

Assembly of the heterodimeric b protein during dikaryon formation in *U. maydis* is concomitant with transient cell cycle arrest as well as with accumulation of phosphorylated forms of Chk1 and translocation of Chk1 into

the nucleus, two hallmarks of Chk1 activation (Mielnichuk et al., 2009). Previous research (Perez-Martin, 2009) established that in response to DNA damage, Chk1 activation results in a G2 cell cycle arrest and involves phosphorylation at two residues (Thr394 and Ser448) located in the regulatory domain (Figure 1A). Mutant isoforms containing alanine in place of these residues could not be activated in response to DNA damage signals (Perez-Martin, 2009). To determine whether these phosphorylation sites were also important during the cell cycle arrest associated with dikaryon formation, we measured the ability of these phosphorylation-refractory Chk1 mutants to support the *b*-induced cell cycle arrest. For this, a *chk1*$^{T394A\ S448A}$ mutant allele tagged with the T7 epitope was integrated at the native locus in AB33 cells, a haploid strain that carry compatible (i. e. able to dimerize) *bE* and *bW* genes under the control of the regulatable *nar1* promoter that is induced by the addition of nitrate to medium (Brachmann et al., 2001). As a control, a T7-tagged wild-type *chk1* allele was used. Upon induction, Chk1$^{T394A\ S448A}$ protein did not show the reduced electrophoretic mobility as observed with wild-type Chk1 protein after induction of heterodimeric b protein (Figure 1B). Moreover, the cells carrying the non-phosphorytable Chk1 allele were impaired in cell cycle arrest just as cells deleted of *chk1* (Figure 1C). We also analyzed the ability of compatible haploid cells carrying the *chk1*$^{T394A\ S448A}$ allele to infect plants, and found that the non-phosphorylatable mutant showed similar virulence defects as those observed in cells lacking Chk1 protein (Figure 1D). In summary, these results show that the *chk1*$^{T394A\ S448A}$ mutant phenocopies all defects observed in the *chk1* null mutant, implying that phosphorylation of

Chk1 at these residues is integral to the mechanism of b-dependent activation of Chk1.

Atr1 is required in the response to DNA damage in *U. maydis*

In other model systems, Chk1 phosphorylation in response to DNA-damage is carried out by two phosphatidylinositol 3-kinase-related kinases (PIKKs), ATM and ATR (Zhou and Elledge, 2000; Nyberg et al., 2002). Putative orthologs of these two PIKKs were present in *U. maydis* genome (Figure 2A). The genes encoding Atm1 (um15011), and Atr1 (um01110) were identified as entries (noted in parenthesis) in the manually annotated MIPS *U. maydis* database (see http://mips.gsf.de/genre/proj/ustilago/). To further analyze the relationships between these putative kinases and Chk1, gene deletion of the corresponding genes was attempted. Constructions containing a hygromycin-resistance cassette flanked by regions located upstream and downstream of the *atr1* and *atm1* ORFs were transformed in haploid cells. Only mutants lacking *atr1* gene were obtained. As this result suggested that *atm1* was essential, a diploid/meiotic analysis protocol was employed. We successfully inactivated one *atm1* allele in the diploid FBD11 strain, replacing it with the hygromycin resistance cassette, generating the *atm1*Δ null allele. After sporulation, we analyzed the meiotic progeny of this strain and we found no hygromycin resistant cells, indicating that *atm1* was an essential gene (not shown). We decided to be focused on the characterization of Atr1. Sequence comparisons of *U. maydis* Atr1 with orthologs from different organisms revealed the presence of conserved domains, including the PIKK-specific domains FAT and FATC (Bosotti et al., 2000) suggesting that *U. maydis* Atr1

is a *bona fide* Atr1 ortholog (Figure 2B). Consistently, we found that cells lacking Atr1 were extremely sensitive to several genotoxic insults: UV irradiation, which makes DNA damages ranging from cyclobutane-pyrimidine dimers to DNA double strand breaks (DSBs); Hydroxyurea (HU), which inhibits ribonucleotide reductase and therefore affects replication by depletion of dNTPs, causing the accumulation of unreplicated forks; Methylmethane sulfonate (MMS), which induces DNA-alkylation; Phleomycine, a radiomimetic drug that causes DSBs on DNA; and IR irradiation, which generate DSBs (Figure 2C). As comparisons we used mutant cells lacking the *chk1* gene as well as cells lacking *brh2*, which encodes a BRCA2-like protein required for homology-directed recombinational repair (Kojic et al., 2002).

Atr1 phosphorylates and activates Chk1 in response to DNA damage in *U. maydis*

To define relationships between *atr1* and *chk1* we constructed double mutants between *chk1* and *atr1* and analyzed sensitivity to UV. As control for this epistasis analysis we also constructed a double *atr1 brh2* mutant strain. Our genetic results suggest that *atr1* acts upstream of *chk1*, since double *chk1 atr1* mutants showed the same sensitivity as *atr1* mutant, while *brh2* seemed to work in a distinct pathway than *atr1* and their effects are additive (Figure 3A).

We also analyzed whether Atr1 was required for the accumulation of phosphorylated forms of Chk1 in response to DNA damage agents. As our current view of DNA-damage dependent Chk1 activation in *U. maydis* is that there are two main signals to be detected by DNA surveillance systems (the

presence of double strand breaks in DNA, induced along this work after phleomycin treatment, and the presence of single strand DNA tracts as hallmark of replication stress, caused by HU treatment), we confronted cultures from wild-type and *atr1* mutant strains carrying the Chk1-T7 allele with HU or phleomycine. We found that absence of Atr1 abolished the mobility shift in the presence of HU, while in the presence of phleomycin, the shift is only partially abrogated. A distinct behavior in Chk1 phosphorylation with respect these two DNA damaging agents was previously noted (Perez-Martin, 2009), suggesting that these two stimuli are transmitted by different cascades, and our results support the idea that at least one of them seems to be totally dependent on Atr1.

Given that phosphorylation seemed to be required for Chk1 activation and that in response to DNA damage Chk1 accumulated in the nucleus, we also analyzed the ability of Chk1 to translocate to nucleus in response to DNA damage in the absence of Atr1. We examined the subcellular localization of a Chk1-GFP allele in the presence of either HU or phleomycine (Figure 3C). While control cells showed a clear nuclear accumulation of the fluorescent signal in the presence of these DNA damaging agents, in the absence of Atr1, Chk1 failed to accumulate in the nucleus, more dramatically in the presence of HU and less obvious in the presence of phleomycin, mirroring the above phosphorylation results (Figure 3D).

Atr1-dependent phosphorylation of Chk1 is required for b-dependent cell cycle arrest

We analyzed whether Atr1 was required for *b*-induced cell cycle arrest. For this, we removed the *atr1* gene in strains expressing compatible *b* proteins (AB33 background). We observed that removal of *atr1* in this genetic background resulted in elongated cells. To distinguish the *b*-induced filaments from such a cell population background, the haploid strains utilized expressed a GFP fusion to a nuclear localization signal under control of the *dik6* promoter, which is specifically activated by the b heterodimer (Flor-Parra et al., 2006). In this way only cells expressing the *b*-dependent program produced a fluorescent nuclear signal. We found that in the control strain almost the totality of *b*-expressing cell population carried a single nucleus, while *chk1*Δ and *atr1*Δ filaments frequently carried more than two nuclei (Figure 4 A, B), which was coherent with a defect in the ability to arrest entry into mitosis. These results suggest that most likely Atr1 is the kinase involved in the activation of Chk1 in response to *b*-induction. To gain additional support to this idea, we investigated whether Atr1 was required for the accumulation of phosphorylated forms of Chk1 in response to the induction of the *b*-dependent program. Consistently we found that there was no Chk1 phosphorylation in cells lacking Atr1 after *b*-induction (Figure 4C).

Atr1 and Chk1 have roles during pathogenic growth in planta

U. maydis infection of maize results in anthocyanin pigment production by the plant and the formation of tumors that are filled with proliferating fungal cells that eventually differentiate into black teliospores (Banuett and Herskowitz, 1996). We tested strains defective either in Chk1 or Atr1 for pathogenicity during the infection process. We found that more than 25 % of the plants

showed no or minor symptoms such as chlorosis (Figure 5A). This result can be easily attributed to impaired formation of a functional infective filament, as a consequence of impaired cell cycle arrest during dikaryon establishment (Mielnichuk et al., 2009). However, once plants were infected with these mutant strains, they rarely showed big tumors, and even in these rare occasions, no teliospores were found in these tumors. A striking feature observed in tumors induced by *chk1*Δ and *atr1*Δ strains is the development of small, shootlike structures (Figure 5B). Such structures were described previously in plants infected by *U. maydis* mutants exhibiting overactivation of cAMP cascade and were attributed to a defective fungal development inside the plant (Kruger et al., 2000).

These results strongly suggest roles of Chk1 and Atr1 beyond the initial steps of infection. A possible explanation for these results might be in the compromised ability of the mutant cells to deal with DNA damage occurring during proliferation inside the plant in response to the plant defense system (i. e. reactive oxygen and/or nitrogen species). However, this explanation seems unlikely since the DNA-damage-sensitive *brh2* mutant cells complete the life cycle at levels similar to wild-type cells (Figure 5A). This suggests that the Atr1 Chk1 axis has some additional role in the pathogenic process beyond signaling repair of DNA damage.

Chk1 and Atr1 are required to maintain the dikaryotic growth

We test whether proliferation inside the plant was affected by the disruption of Atr1-Chk1. Infected plant tissue was stained with Alexa-Fluor labeled wheat germ agglutinin (WGA-AF488), a lectin that binds to chitin enabling detection

of fungal cell walls, and with propidium iodide, to visualize plant membranes (Doehlemann et al., 2009). *U. maydis* grows as a dikaryon during its pathogenic state. Previous work (Scherer et al., 2006) showed that clamp-like structures were involved in the distribution of nuclei in hyphae, and thereby in the ability to proliferate inside plant. Consistently, we found that in wild-type and *brh2*Δ filaments a single clamp-like structures was placed at the position of septum formation. However, *atr1*Δ and *chk1*Δ mutants were impaired in proliferation, and hyphae showed aberrant formation and variable distribution of clamp-like structures (Figures 6A and B). We tried to quantify these defects and for this, individual hyphae were counted and sorted in function of the number of clamp-like structures observed at the three more apical septa (Figure 7A). Wild-type and *brh2*Δ filaments showed the expected distribution of one clamp-like structure per septum. However, filaments defective in *chk1* or *atr1* showed a clear deviation of this pattern, showing apical septa that carry more than one clamp-like structure.

Since formation of clamp-like structures are directly related to the process of nuclear division, we wondered whether nuclear distribution was also affected by the disruption of Atr1 or Chk1. To visualize fungal nuclei in infected plant we used strains carrying a triple GFP gene fused to a nuclear localization sequence under the control of the constitutive promoter P_{tef1} (Flor-Parra et al., 2006). While wild-type and *brh2*Δ filaments carried two nuclei per cellular compartment, *atr1*Δ and *chk1*Δ mutants carried variable combinations from 1 to 4 (Figures 7B and C). These observations suggest that Chk1 and Atr1 have roles in appropriate nuclear segregation and therefore in their absence

dikaryotic cells replicate aberrantly, most likely causing the observed proliferation defects *in planta*.

DISCUSSION

Dikaryon cell division involves nuclear migration and sorting of the divided nuclei to ensure that each daughter cell inherits a balance of each parental genome (Casselton, 2002). This cell cycle relies on a synchronized nuclear division and the development of clamp connections, a specialized projection formed close to the position of the future septum formation. One nucleus enters and divides in the developing clamp cell, whereas the other divides in the main hypha, with the result that mitosis occurs in two distinct cell compartments. It is not known in which cell cycle stage these processes take place, however most likely will be G2 phase, as it happens after nuclear DNA duplication and before mitosis. Moreover, the movement of one of the nucleus into clamp cell is reminiscent of the movement of diploid nucleus into the daughter bud during vegetative cell division in *U. maydis*, a process occurring in G2/M transition (Straube et al., 2005). Such a nuclear “ballet” most likely will need an extended G2 period to proceed. One of the roles of Atr1-Chk1 axis during DNA damage response is to provide an elongated G2 phase to cells to give time to solve the problems before mitosis start (Toettcher et al., 2009). On this basis, we propose that the role of Atr1-Chk1 axis during the dikaryotic cell cycle is to synchronize nuclei as well as to provide an extended window during G2 phase to enable the above-mentioned process (Figure 8). It could be well that in the absence of Atr1-Chk1, the nuclear cycle, clamp cell

formation and cytokinesis occur asynchronously resulting in the defects such as observed in mutant hyphae inside the plant.

Since b proteins are required for synchronization between cell cycle and cytokinesis (Wahl et al., 2010), we propose that in normal conditions it is the timely activation of Atr1-Chk1 axis by the b homeodomain protein that produces accurate control of cell cycle. We have no clue about how the b-protein activates this cascade. Our preliminary attempts to correlate expression of compatible *b* alleles and increase in *chk1* or *atr1* transcription were negative (not shown). Chk1 activation is linked to DNA damage in vegetative cells and our results indicated that Atr1 is also required for response to DNA damage. Therefore it is tempting to speculate that *b*-induction could be associated with some class of DNA damage that triggers this kinase cascade during b-dependent filament formation. It is worth noting that b proteins activate the transcription of a gene encoding a putative DNA polymerase β (Brachmann et al., 2001), which belongs to the family X of DNA polymerases that are described to be involved in a number of DNA repair processes (Ramadan et al., 2004). On the other hand, several lines of evidence suggest that it is unlikely that activation of Atr1-Chk1 cascade during *b*-induction is related to DNA damage. First, in previous studies using the formation of Rad51 foci as reporter for active DNA repair, there was no evidence for presence of DNA damage associated with the induction of the infective hyphae (Mielnichuk et al., 2009). Second, we observed no defect in the ability to arrest cell cycle (not shown) or to infect plants (Figure 5A) in cells lacking Brh2, which is required for DNA repair by homologous recombination (Kojic et al., 2002). Finally, preliminary research indicated that cells lacking

the PolX polymerase were able to arrest cell cycle at levels comparable to wild-type cells (not shown). Two recent reports showed that activation of DNA damage response cascade can be triggered in the absence of DNA damage by stable association of elements of the cascade with chromatin (Bonilla et al., 2008; Soutoglou and Misteli, 2008). Whether a similar mechanism could explain our observations in *U. maydis* will need additional research.

There are increasing numbers of reports indicating that the ability of DNA damage response cascade to modulate cell cycle progression can be used during developmental processes. Some of these processes were linked with limited DNA damage as it happens in B cell differentiation (Sherman et al., 2010) or even in the absence of apparent DNA damage, such as in the midblastula transition in *Drosophila* embryos (Sibon et al., 1997) or in the asynchronous division at two-cell-stage *C. elegans* embryos (Brauchle et al., 2003). The surprising finding that a regulatory cascade involved in DNA damage responses plays a role in a fungal developmental process mirrors these previous results and reinforces the emerging idea that checkpoint cascades may have roles beyond cell surveillance by virtue of their ability to interact with cell cycle machinery.

METHODS

U. maydis genetic methods

U. maydis strains are listed in Table 1. Manipulations with *U. maydis*, culture methods, gene disruption and gene transfer procedures, survival after DNA damage, plant infections, protein extracts, immunoprecipitations and Western analysis have been described previously (see (Mielnichuk et al., 2009) and

references therein). Null mutants were constructed by replacing the entire open reading frames with cassettes expressing resistance to antibiotics by standard methodology. Briefly a pair of DNA fragments flanking the *atr1* ORF were amplified and ligated to a gene cassette encoding hygromycin resistance and flanked by *Sfi*I sites. The 5' fragment spans from nucleotide -1967 to nucleotide -29 (considering the adenine in the ATG as nucleotide +1) and it was produced by PCR amplification using the primers ATR1-22 (5'TTAATTAAGCAGATCCACTGCTGAACGGGTTTC3') and ATR1-3 (5'GGTGGCCATCTAGGCCTTCCTTAGGCTTGGACACTGGAGATCAGT3'). The flanking 3' fragment was obtained after PCR amplification with primers ATR1-4 (5'ATAGGCCTGAGTGGCCACGGTTTGCAGCTGCATACAGTAGGATAT3') and ATR1-23 (5'TTAATTAAGGAACTCATCAGCGTGTGGAACCGA3') and spans from nucleotide +7912 to nucleotide +9962

Microscopy. To visualize fungal hyphae in plant by WGA-AF488 (Invitrogen) and Propidium Iodide (Sigma), samples 2-3 days post infection of maize leaves were incubated in staining solution (1 µg/ml Propidium iodide, 10 µg/ml WGA-AF488, 0.02% Tween20) for 30 minutes and washed in 1x PBS (pH=7.4) (Doehlemann et al., 2009). Analysis of the infection stages was done using a Deltavision widefield microscope (Applied Precision). Image deconvolution was performed using z-series of between 10 and 15 focal planes, acquired at 0.5-µm intervals. Image processing was performed using Adobe Photoshop CS2 and Canvas 8.0 (Deneba)

To quantify the clamp-like structures in fungal hyphae, plant leaves 2-3 days post infections were analyzed. Individual hyphae where could be observed the hyphal tip as well as the penetration points were analyzed quantifying the number of clamp-like structures. To quantify the number of nuclei per cellular compartment maize leaves 2-3 days post infections were analyzed. Only nuclei in individual hyphae were quantified.

ACKNOWLEDGMENTS

We thank Prof. Lorraine Symington (Columbia University) for stimulating discussions. CdS was supported by FPI contract. This work was supported by a Grant from the Spanish Government (BIO2008-04054).

LEGENDS TO FIGURES

Figure 1. A *chk1* allele refractory to phosphorylation mimics the *chk1*Δ loss of function mutation with respect b-dependent filament cell cycle arrest and *in planta* proliferation.

(A) Scheme of Chk1 showing the two phosphorytable residues required for Chk1 activation.

(B) *In vivo* phosphorylation of Chk1 during *b*-dependent filamentation. AB33-derived cells carrying an endogenous *chk1-T7* (control, UCS31) or the *chk1*$^{T394A\ S448A}$ allele (UMP183) were incubated in MM-NO_3 for the indicated time (in hours). Protein extracts were immunoprecipitated with a commercial anti-T7 antibody and immunoprecipitates were subjected to SDS-PAGE and immunoblotted with anti-T7 antibody.

(C) AB33 (control, UCS31) and derivated strains lacking the *chk1* gene (*chk1*Δ, UMP114) or carrying the *chk1*$^{T394A\ S448A}$ allele (UMP183) were incubated in inducing conditions (MM-NO_3). Cells were stained with DAPI to detect nuclei. Graphic shows the percentage cells producing mononucleated filaments (i. e. cell-cycle arrested) after 24 hours of incubation; means and standard deviations are shown.

(D) Quantification of symptoms in maize plants after 14 days post-infection with wild-type (control, UCM350xUCM520), *chk1*Δ (UMP122xUMP129) or *chk1*$^{T394A\ S448A}$ (UMP190xUMP191) mutant crosses.

Figure 2. *Ustilago maydis* Atr1.

(A) Dendrogram of characterized Atr1 and Atm1-like proteins proteins. The tree was reconstructed using the ClustalW method (http://www.ebi.ac.uk/clustalw/). The proteins utilized were *Homo sapiens* ATR (CAA70298.1) and ATM (AAB38309.1); *Schizosaccharomyces pombe*; Rad3 (SPBC216.05), and Tel1 (SPCC23B6.03c); *Saccharomyces cerevisiae* Mec1 (YBR136W), and Tel1 (YBL088C); *Aspergillus nidulans* AtmA (AN0038.2) and UvsB (AN6975.2); and *Ustilago maydis* um15011 (Atm1) and Um01110 (Atr1)

(B) Schematic representation of the domain architecture of Atr1 proteins in different organisms.

(C) Sensitivity of cells lacking *atr1* gene (UCS9) in comparison to wild-type (UCM350), *chk1*Δ (UMP122) and *brh2*Δ (UCM565) cells to different chemicals as well as IR and UV irradiation. Cell suspensions were spotted onto agar plates contained the indicated drugs (HU, hydroxyurea; Phleo, phleomycin;

MMS, methyl methanesulfonate). For UV ad IR sensitivity, cells were irradiated at the indicated dose after being spotted. The spots were photographed after incubation for 2 days.

Figure 3. Atr1 is required for activation of Chk1 in response to DNA damage in *U. maydis*.

(A) Epistatic analysis between *chk1*, *atr1* and *brh2*. Survival curves against UV irradiation of the indicated single and double mutants were obtained. Cells were grown to late log phase, adjusted to a density of $2x10^7$ cells per ml and irradiated with UV. Survival was determined by counting colonies visible after incubation for 2 to 3 days.

(C) *In vivo* phosphorylation of Chk1 in response to agents that induce DNA-damage depends on Atr1. Wild-type (wt, UMP162) and *atr1*Δ (UMP207) cells carrying an endogenous Chk1-T7 allele were grown in the presence of none (control), 0.5 mM hydroxyurea or 50 ng/ml phleomycin (Phleo) for 6 hours. Protein extracts were immunoprecipitated with a commercial anti-T7 antibody and immunoprecipitates were subjected to SDS-PAGE and immunoblotted with anti-T7 antibody.

(C) Atr1 was required to localize Chk1 at the nucleus. Cell images of wild-type (wt, UMP111) and *atr1*Δ strain (UCS15) carrying a Chk1-3GFP fusion protein after 3 hours of incubation in the presence of hydroxyurea (HU) or phleomycin (Phleo). Bar: 10 μm.

(D) Quantification of the cell response to DNA damage as the percentage of cells carrying a clear nuclear GFP fluorescence signal.

Figure 4. Atr1 is required for b-dependent cell cycle arrest

(A) Cell images of control (UCS20) and a derivate strain lacking the *chk1* gene (*chk1*Δ, UMP112) or atr1 (*atr1*Δ, UCS21) incubated for 8 hours in inducing conditions (MM-NO_3). Strains carried a NLS-GFP fusion under control of the *b*-dependent *dik6* promoter to detect nucleus. Bar: 15 μm.

(B) Percentage of cells producing mononucleated filaments (i. e. cell-cycle arrested) after 24 hours of incubation; means and standard deviations are shown.

(C) Dependence on *atr1* for *In vivo* phosphorylation of Chk1 during *b*-dependent filamentation. Control (UCS31) and *atr1*Δ (UCS32) AB33-derived cells carrying an endogenous *chk1-T7* allele were incubated in MM-NO_3 for the indicated time (in hours). Protein extracts were immunoprecipitated with a commercial anti-T7 antibody and immunoprecipitates were subjected to SDS-PAGE and immunoblotted with anti-T7 antibody.

Figure 5. Atr1 and Chk1 are required for full virulence in *U. maydis*

(A) Quantification of symptoms in maize plants after 14 days post-infection with crosses of wild-type (control, UCM350xUCM520) *brh2*Δ (UCM565xUCM575), *chk1*Δ (UMP122xUMP129) and *atr1*Δ (UCS9xUCS10) strains.

(B) Morphology of tumors caused by wild-type (control) and compatible combinations of *brh2*Δ, *chk1*Δ and *atr1*Δ strains. Representative tumors were photographed 16 days postinfection. Arrows mark shootlike structures.

Figure 6. Atr1 and Chk1 are required for *in planta* apropriated proliferation.

(A) Images of plant tissues 2 days post infection with the indicated crosses of fungal cells. Hyphae (stained by WGA-AF488; green) grow intracellularly in epidermal cells of maize (stained by propidium iodide; red). Arrows mark clamp-like connections. Bar: 10 μm.

(B) Examples of aberrant hyphal morphologies found in *chk1*Δ and *atr1*Δ filaments *in planta*. Asterisk marks the hyphal tip. Arrows pointed aberrant clamp-like structures.

Figure 7. Atr1 and Chk1 are required for dikaryon maintenance *in planta*.

(A) Distribution of clamp-like structures in mutant cells. Infected plant tissue with the indicated strains was stained with WGA-AF488 and PI. Then individual hyphae were counted and sorted in function of the number of clamp-like structures observed at the three more apical septa (S1, S2 and S3). Control (wild-type) and *brh2*Δ filaments showed the expected distribution of one clamp-like structure per septum. Filaments defective in *chk1* or *atr1* showed a clear deviation of this pattern. Means and standard deviations are shown. Upper images exemplify typical wild-type (left) or mutant (right) hyphae.

(B) Examples of wild-type and the indicated mutant hyphae expressing a nuclear localized 3xGFP to detect nuclei. Wild-type hyphae contain two nuclei per cell as observed for *brh2*Δ. The *atr1*Δ and *chk1*Δ hyphae contain multiple nuclei per cell compartment. The distribution of the nuclei with respect to the clamp-like structures is given in the lateral illustrations.

(C) Quantification of the number of nuclei per cellular compartment in hyphae from infected plant tissue with the indicated strains. Means and standard deviations are shown.

Figure 8. Working model of the role of Atr1-Chk1 axis during dikaryotic cell cycle. See text for description.

References

Banuett, F., and Herskowitz, I. (1996). Discrete developmental stages during teliospore formation in the corn smut fungus, Ustilago maydis. Development **122,** 2965-2976.

Bonilla, C.Y., Melo, J.A., and Toczyski, D.P. (2008). Colocalization of sensors is sufficient to activate the DNA damage checkpoint in the absence of damage. Mol Cell **30,** 267-276.

Bosotti, R., Isacchi, A., and Sonnhammer, E.L. (2000). FAT: a novel domain in PIK-related kinases. Trends Biochem Sci **25,** 225-227.

Brachmann, A., Weinzierl, G., Kamper, J., and Kahmann, R. (2001). Identification of genes in the bW/bE regulatory cascade in Ustilago maydis. Mol Microbiol **42,** 1047-1063.

Brauchle, M., Baumer, K., and Gonczy, P. (2003). Differential activation of the DNA replication checkpoint contributes to asynchrony of cell division in C. elegans embryos. Curr Biol **13,** 819-827.

Brefort, T., Doehlemann, G., Mendoza-Mendoza, A., Reissmann, S., Djamei, A., and Kahmann, R. (2009). Ustilago maydis as a Pathogen. Annu Rev Phytopathol **47,** 423-445.

Brown, A.J., and Casselton, L.A. (2001). Mating in mushrooms: increasing the chances but prolonging the affair. Trends Genet **17,** 393-400.

Casselton, L.A. (2002). Mate recognition in fungi. Heredity **88,** 142-147.

Casselton, L.A., and Olesnicky, N.S. (1998). Molecular genetics of mating recognition in basidiomycete fungi. Microbiol Mol Biol Rev **62,** 55-70.

Chen, E.H., Grote, E., Mohler, W., and Vignery, A. (2007). Cell-cell fusion. FEBS Lett **581,** 2181-2193.

Chen, Y., and Sanchez, Y. (2004). Chk1 in the DNA damage response: conserved roles from yeasts to mammals. DNA Repair (Amst) **3,** 1025-1032.

Clark, T.A., and Anderson, J.B. (2004). Dikaryons of the basidiomycete fungus Schizophyllum commune: evolution in long-term culture. Genetics **167,** 1663-1675.

Doehlemann, G., van der Linde, K., Assmann, D., Schwammbach, D., Hof, A., Mohanty, A., Jackson, D., and Kahmann, R. (2009). Pep1, a secreted effector protein of Ustilago maydis, is required for successful invasion of plant cells. PLoS Pathog **5,** e1000290.

Feldbrugge, M., Kamper, J., Steinberg, G., and Kahmann, R. (2004). Regulation of mating and pathogenic development in Ustilago maydis. Curr Opin Microbiol **7,** 666-672.

Flor-Parra, I., Vranes, M., Kamper, J., and Perez-Martin, J. (2006). Biz1, a zinc finger protein required for plant invasion by Ustilago maydis, regulates the levels of a mitotic cyclin. Plant Cell **18,** 2369-2387.

Gladfelter, A., and Berman, J. (2009). Dancing genomes: fungal nuclear positioning. Nat Rev Microbiol **7,** 875-886.

Ikeda, K., Nakamura, H., and Matsumoto, N. (2003). Mycelial incompatibility operative in pairings between single basidiospore isolates of Helicobasidium mompa. Mycol Res **107,** 847-853.

Kojic, M., Kostrub, C.F., Buchman, A.R., and Holloman, W.K. (2002). BRCA2 homolog required for proficiency in DNA repair, recombination, and genome stability in Ustilago maydis. Mol Cell **10,** 683-691.

Kruger, J., Loubradou, G., Wanner, G., Regenfelder, E., Feldbrugge, M., and Kahmann, R. (2000). Activation of the cAMP pathway in Ustilago maydis reduces fungal proliferation and teliospore formation in plant tumors. Mol Plant Microbe Interact **13,** 1034-1040.

Kues, U. (2000). Life history and developmental processes in the basidiomycete Coprinus cinereus. Microbiol Mol Biol Rev **64,** 316-353.

Lee, S.C., Ni, M., Li, W., Shertz, C., and Heitman, J. (2010). The evolution of sex: a perspective from the fungal kingdom. Microbiol Mol Biol Rev **74,** 298-340.

Mielnichuk, N., Sgarlata, C., and Perez-Martin, J. (2009). A role for the DNA-damage checkpoint kinase Chk1 in the virulence program of the fungus Ustilago maydis. J Cell Sci **122,** 4130-4140.

Nyberg, K.A., Michelson, R.J., Putnam, C.W., and Weinert, T.A. (2002). Toward maintaining the genome: DNA damage and replication checkpoints. Annu Rev Genet **36,** 617-656.

Perez-Martin, J. (2009). DNA-damage response in the basidiomycete fungus Ustilago maydis relies in a sole Chk1-like kinase. DNA Repair (Amst) **8,** 720-731.

Ramadan, K., Shevelev, I., and Hubscher, U. (2004). The DNA-polymerase-X family: controllers of DNA quality? Nat Rev Mol Cell Biol **5,** 1038-1043.

Scherer, M., Heimel, K., Starke, V., and Kamper, J. (2006). The Clp1 protein is required for clamp formation and pathogenic development of Ustilago maydis. Plant Cell **18,** 2388-2401.

Sherman, M.H., Kuraishy, A.I., Deshpande, C., Hong, J.S., Cacalano, N.A., Gatti, R.A., Manis, J.P., Damore, M.A., Pellegrini, M., and Teitell, M.A. (2010). AID-induced genotoxic stress promotes B cell differentiation in the germinal center via ATM and LKB1 signaling. Mol Cell **39,** 873-885.

Sibon, O.C., Stevenson, V.A., and Theurkauf, W.E. (1997). DNA-replication checkpoint control at the Drosophila midblastula transition. Nature **388,** 93-97.

Soutoglou, E., and Misteli, T. (2008). Activation of the cellular DNA damage response in the absence of DNA lesions. Science **320,** 1507-1510.

Straube, A., Weber, I., and Steinberg, G. (2005). A novel mechanism of nuclear envelope break-down in a fungus: nuclear migration strips off the envelope. EMBO J **24,** 1674-1685.

Toettcher, J.E., Loewer, A., Ostheimer, G.J., Yaffe, M.B., Tidor, B., and Lahav, G. (2009). Distinct mechanisms act in concert to mediate cell cycle arrest. Proc Natl Acad Sci U S A **106,** 785-790.

Wahl, R., Zahiri, A., and Kamper, J. (2010). The Ustilago maydis b mating type locus controls hyphal proliferation and expression of secreted virulence factors in planta. Mol Microbiol **75,** 208-220.

Zhou, B.B., and Elledge, S.J. (2000). The DNA damage response: putting checkpoints in perspective. Nature **408,** 433-439.

Table 1. Strains utilized in this work

Strain	Relevant Genotype	Reference
UCM350	*a1b1*	Holliday, 1991
UCM520	*a2b2*	Holliday, 1991
UMP122	*a1b1 chk1*Δ	Pérez-Martín, 2009
UMP129	*a2b2 chk1*Δ	Mielnichuk et al 2009
UCS9	*a1b1 atr1*Δ	This work
UCS10	*a2b2 atr1*Δ	This work
UCM565	*a1b1 brh2*Δ	Kojic et al 2002
UCM575	*a2b2 brh2*Δ	Kojic et al 2002
UCS22	*a1b1 atr1*Δ *chk1*Δ	This work
UCS27	*a1b1 atr1*Δ *brh2*Δ	This work
AB33	*a2* P_{nar1}*:bW2* P_{nar1}*:bE1*	Brachmann et al., 2001
UCS31	*a2* P_{nar1}*:bW2* P_{nar1}*:bE1 chk1-T7*	This work
UMP114	*a2* P_{nar1}*:bW2* P_{nar1}*:bE1 chk1*Δ	Mielnichuk et al 2009
UCS32	*a2* P_{nar1}*:bW2* P_{nar1}*:bE1 chk1-T7 atr1*Δ	This work
UMP183	*a2* P_{nar1}*:bW2* P_{nar1}*:bE1 chk1-T7*$^{T394A\ S448A}$	This work
UMP190	*a1b1 chk1-T7*$^{T394A\ S448A}$	This work
UMP191	*a2b2 chk1-T7*$^{T394A\ S448A}$	This work
UMP162	*a1b1 chk1-T7*	This work
UMP207	*a1b1 atr1*Δ *chk1-T7*	This work
UMP111	*a1b1 chk1-3GFP*	Pérez-Martín, 2009
UCS15	*a1b1 atr1*Δ *chk1-3GFP*	This work
UCS20	*a2* P_{nar1}*:bW2* P_{nar1}*:bE1* P_{dik6}*:NLS-3GFP*	This work
UMP112	*a2* P_{nar1}*:bW2* P_{nar1}*:bE1* P_{dik6}*:NLS-3GFP chk*1Δ	Mielnichuk et al 2009
UCS21	*a2* P_{nar1}*:bW2* P_{nar1}*:bE1* P_{dik6}*:NLS-3GFP atr1*Δ	This work
UMP196	*a1 b1* P_{tef1}*:NLS-3GFP*	This work
UMP197	*a1 b1* P_{tef1}*:NLS-3GFP brh2*Δ	This work
UMP198	*a1 b1* P_{tef1}*:NLS-3GFP atr1*Δ	This work
UMP199	*a1 b1* P_{tef1}*:NLS-3GFP chk1*Δ	This work

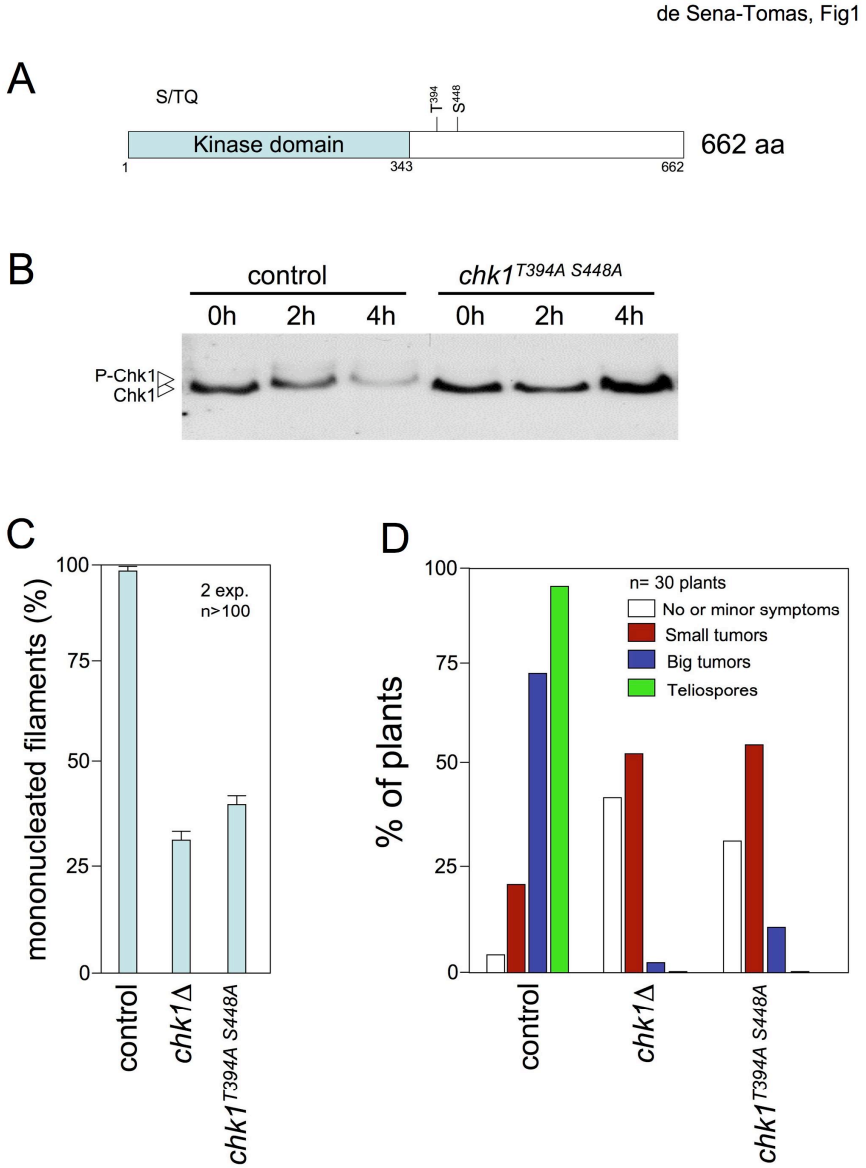

Figure 1. A *chk1* allele refractory to phosphorylation mimics the *chk1*Δ loss of function mutation with respect b-dependent filament cell cycle arrest and *in planta* proliferation.
(A) Scheme of Chk1 showing the two phosphorytable residues required for Chk1 activation.
(B) *In vivo* phosphorylation of Chk1 during *b*-dependent filamentation. AB33-derived cells carrying an endogenous *chk1-T7* (control, UCS31) or the *chk1*$^{T394A\ S448A}$ allele (UMP183) were incubated in MM-NO_3 for the indicated time (in hours). Protein extracts were immunoprecipitated with a commercial anti-T7 antibody and immunoprecipitates were subjected to SDS-PAGE and immunoblotted with anti-T7 antibody.
(C) AB33 (control, UCS31) and derivated strains lacking the *chk1* gene (*chk1*Δ, UMP114) or carrying the *chk1*$^{T394A\ S448A}$ allele (UMP183) were incubated in inducing conditions (MM-NO_3). Cells were stained with DAPI to detect nuclei. Graphic shows the percentage cells producing mononucleated filaments (i. e. cell-cycle arrested) after 24 hours of incubation; means and standard deviations are shown.
(D) Quantification of symptoms in maize plants after 14 days post-infection with wild-type (control, UCM350xUCM520), *chk1*Δ (UMP122xUMP129) or *chk1*$^{T394A\ S448A}$ (UMP190xUMP191) mutant crosses.

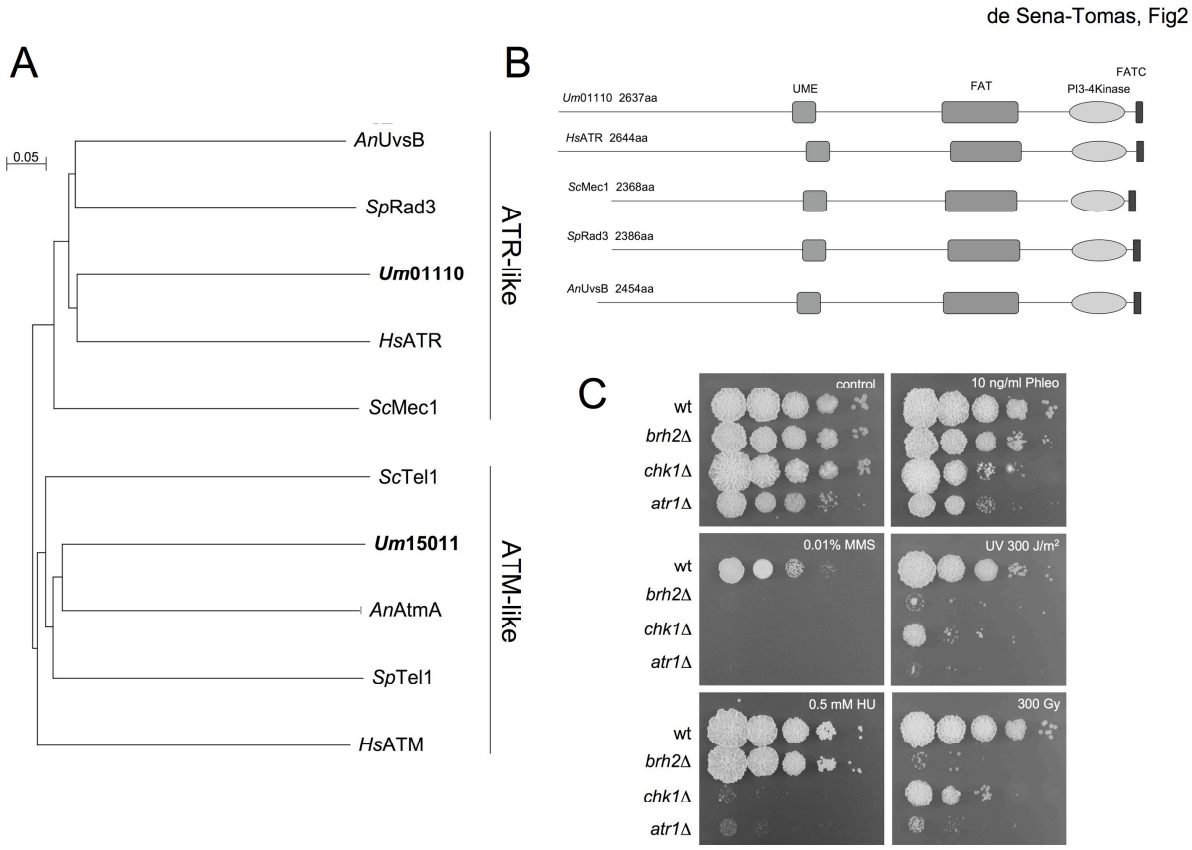

Figure 2. *Ustilago maydis* Atr1.
(A) Dendrogram of characterized Atr1 and Atm1-like proteins proteins. The tree was reconstructed using the ClustalW method (http://www.ebi.ac.uk/clustalw/). The proteins utilized were *Homo sapiens* ATR (CAA70298.1) and ATM (AAB38309.1); *Schizosaccharomyces pombe*; Rad3 (SPBC216.05), and Tel1 (SPCC23B6.03c); *Saccharomyces cerevisiae* Mec1 (YBR136W), and Tel1 (YBL088C); *Aspergillus nidulans* AtmA (AN0038.2) and UvsB (AN6975.2); and *Ustilago maydis* um15011 (Atm1) and Um01110 (Atr1)
(B) Schematic representation of the domain architecture of Atr1 proteins in different organisms.
(C) Sensitivity of cells lacking *atr1* gene (UCS9) in comparison to wild-type (UCM350), *chk1*Δ (UMP122) and *brh2*Δ (UCM565) cells to different chemicals as well as IR and UV irradiation. Cell suspensions were spotted onto agar plates contained the indicated drugs (HU, hydroxyurea; Phleo, phleomycin; MMS, methyl methanesulfonate). For UV ad IR sensitivity, cells were irradiated at the indicated dose after being spotted. The spots were photographed after incubation for 2 days.

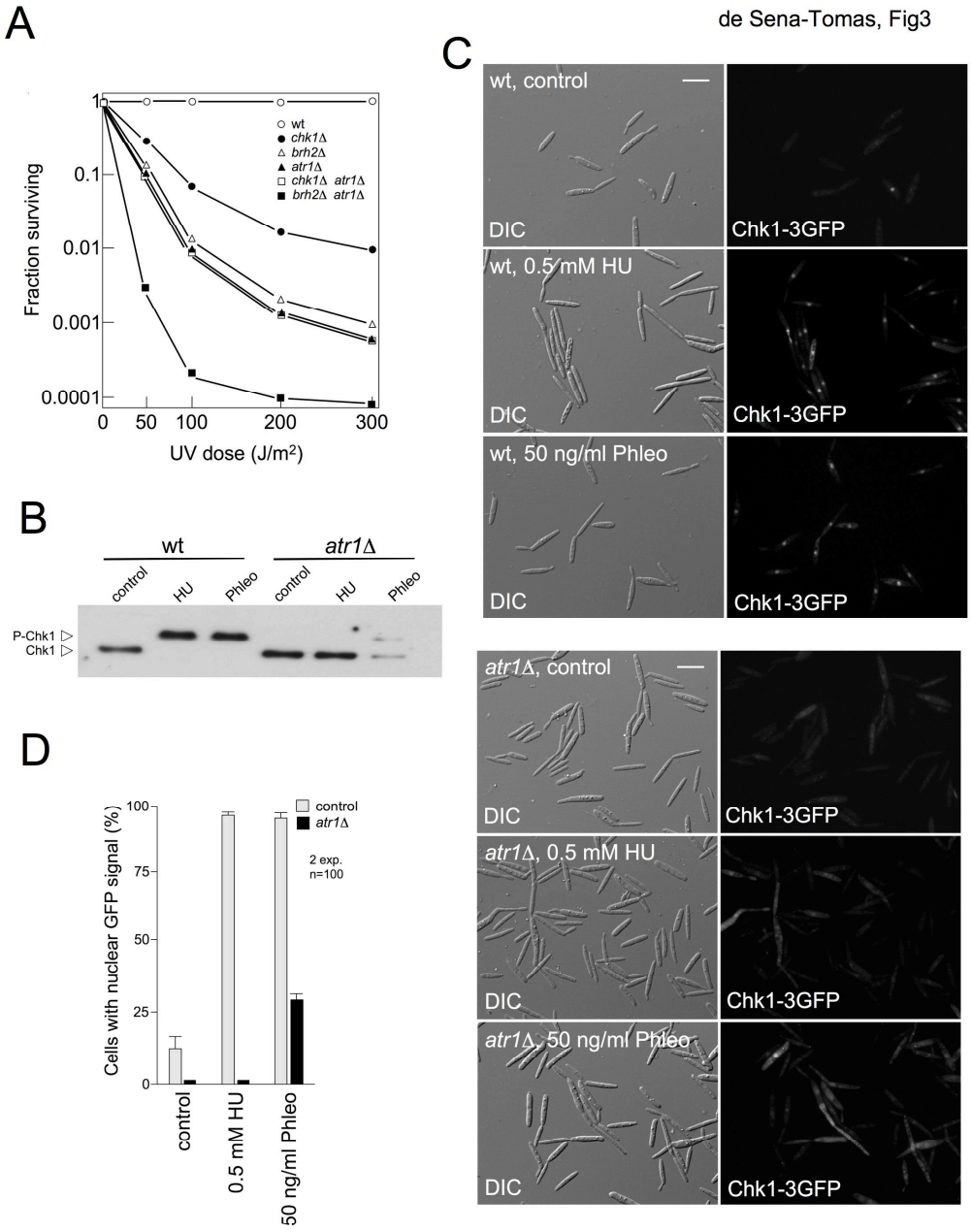

Figure 3. Atr1 is required for activation of Chk1 in response to DNA damage in *U. maydis*.
(A) Epistatic analysis between *chk1*, *atr1* and *brh2*. Survival curves against UV irradiation of the indicated single and double mutants were obtained. Cells were grown to late log phase, adjusted to a density of $2x10^7$ cells per ml and irradiated with UV. Survival was determined by counting colonies visible after incubation for 2 to 3 days.
(C) *In vivo* phosphorylation of Chk1 in response to agents that induce DNA-damage depends on Atr1. Wild-type (wt, UMP162) and *atr1*Δ (UMP207) cells carrying an endogenous Chk1-T7 allele were grown in the presence of none (control), 0.5 mM hydroxyurea or 50 ng/ml phleomycin (Phleo) for 6 hours. Protein extracts were immunoprecipitated with a commercial anti-T7 antibody and immunoprecipitates were subjected to SDS-PAGE and immunoblotted with anti-T7 antibody.
(C) Atr1 was required to localize Chk1 at the nucleus. Cell images of wild-type (wt, UMP111) and *atr1*Δ strain (UCS15) carrying a Chk1-3GFP fusion protein after 3 hours of incubation in the presence of hydroxyurea (HU) or phleomycin (Phleo). Bar: 10 μm.
(D) Quantification of the cell response to DNA damage as the percentage of cells carrying a clear nuclear GFP fluorescence signal.

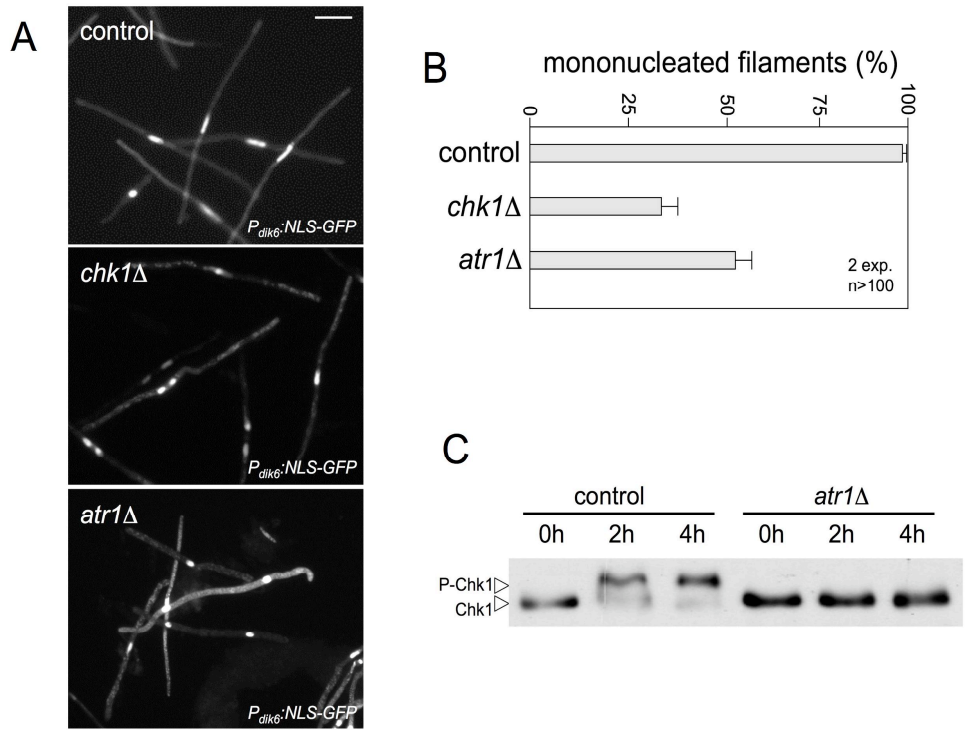

Figure 4. Atr1 is required for b-dependent cell cycle arrest
(A) Cell images of control (UCS20) and a derivate strain lacking the *chk1* gene (*chk1*Δ, UMP112) or atr1 (*atr1*Δ, UCS21) incubated for 8 hours in inducing conditions (MM-NO_3). Strains carried a NLS-GFP fusion under control of the *b*-dependent *dik6* promoter to detect nucleus. Bar: 15 μm.
(B) Percentage of cells producing mononucleated filaments (i. e. cell-cycle arrested) after 24 hours of incubation; means and standard deviations are shown.
(C) Dependence on *atr1* for *In vivo* phosphorylation of Chk1 during *b*-dependent filamentation. Control (UCS31) and *atr1*Δ (UCS32) AB33-derived cells carrying an endogenous *chk1-T7* allele were incubated in MM-NO_3 for the indicated time (in hours). Protein extracts were immunoprecipitated with a commercial anti-T7 antibody and immunoprecipitates were subjected to SDS-PAGE and immunoblotted with anti-T7 antibody.

de Sena-Tomas, Fig 5

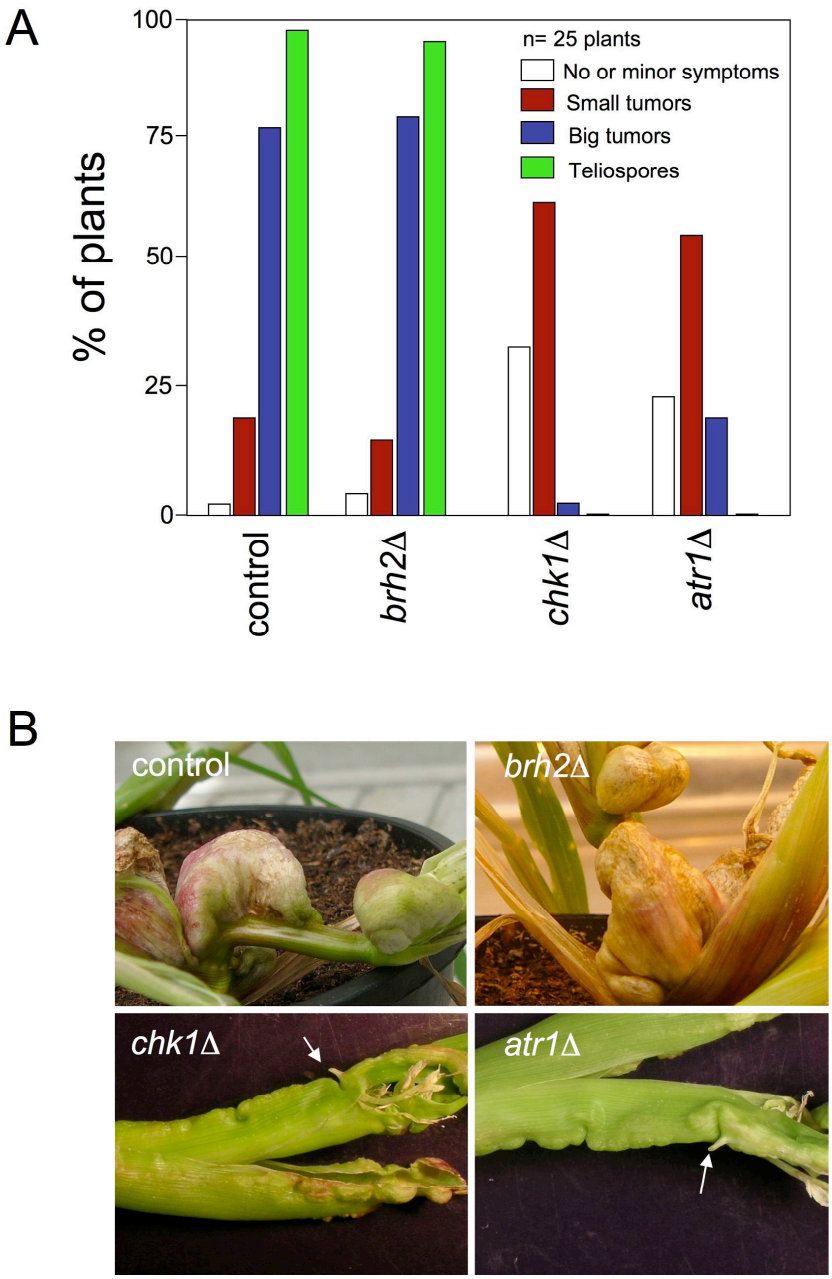

Figure 5. Atr1 and Chk1 are required for full virulence in *U. maydis*
(A) Quantification of symptoms in maize plants after 14 days post-infection with crosses of wild-type (control, UCM350xUCM520) *brh2*Δ (UCM565xUCM575), *chk1*Δ (UMP122xUMP129) and *atr1*Δ (UCS9xUCS10) strains.
(B) Morphology of tumors caused by wild-type (control) and compatible combinations of *brh2*Δ, *chk1*Δ and *atr1*Δ strains. Representative tumors were photographed 16 days postinfection. Arrows mark shootlike structures.

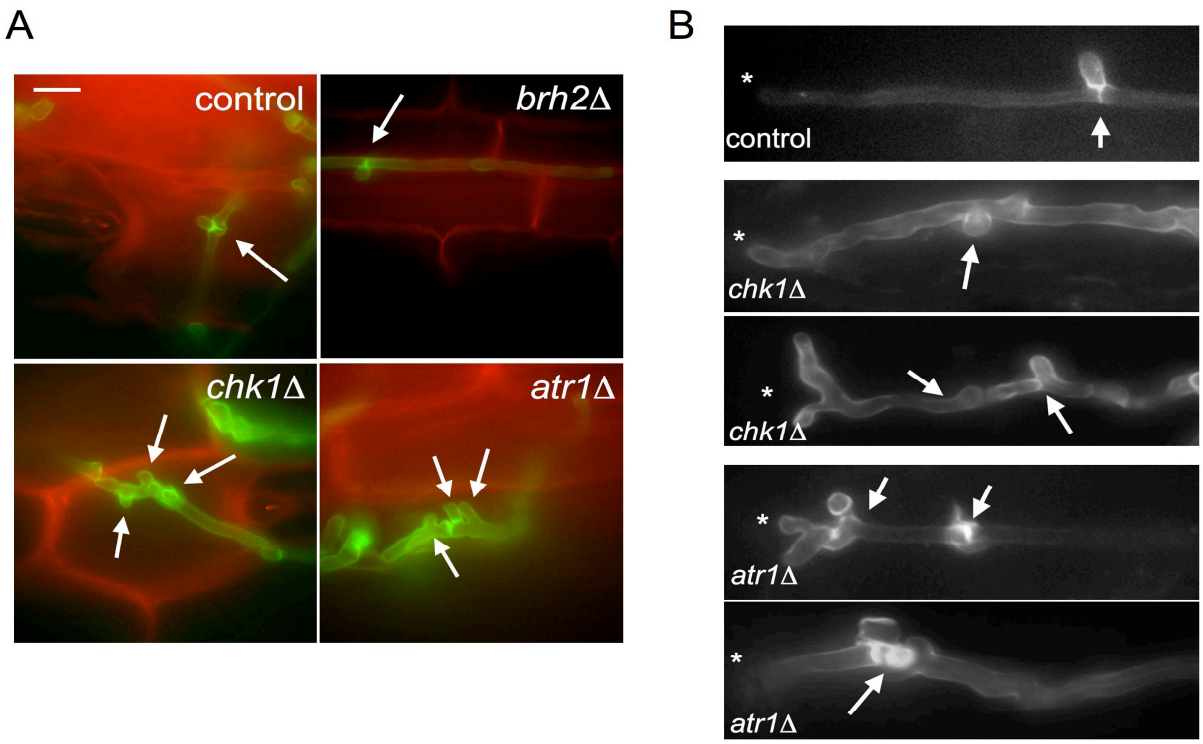

Figure 6. Atr1 and Chk1 are required for *in planta* apropriated proliferation.
(A) Images of plant tissues 2 days post infection with the indicated crosses of fungal cells. Hyphae (stained by WGA-AF488; green) grow intracellularly in epidermal cells of maize (stained by propidium iodide; red). Arrows mark clamp-like connections. Bar: 10 μm.
(B) Examples of aberrant hyphal morphologies found in *chk1*Δ and *atr1*Δ filaments *in planta*. Asterisk marks the hyphal tip. Arrows pointed aberrant clamp-like structures.

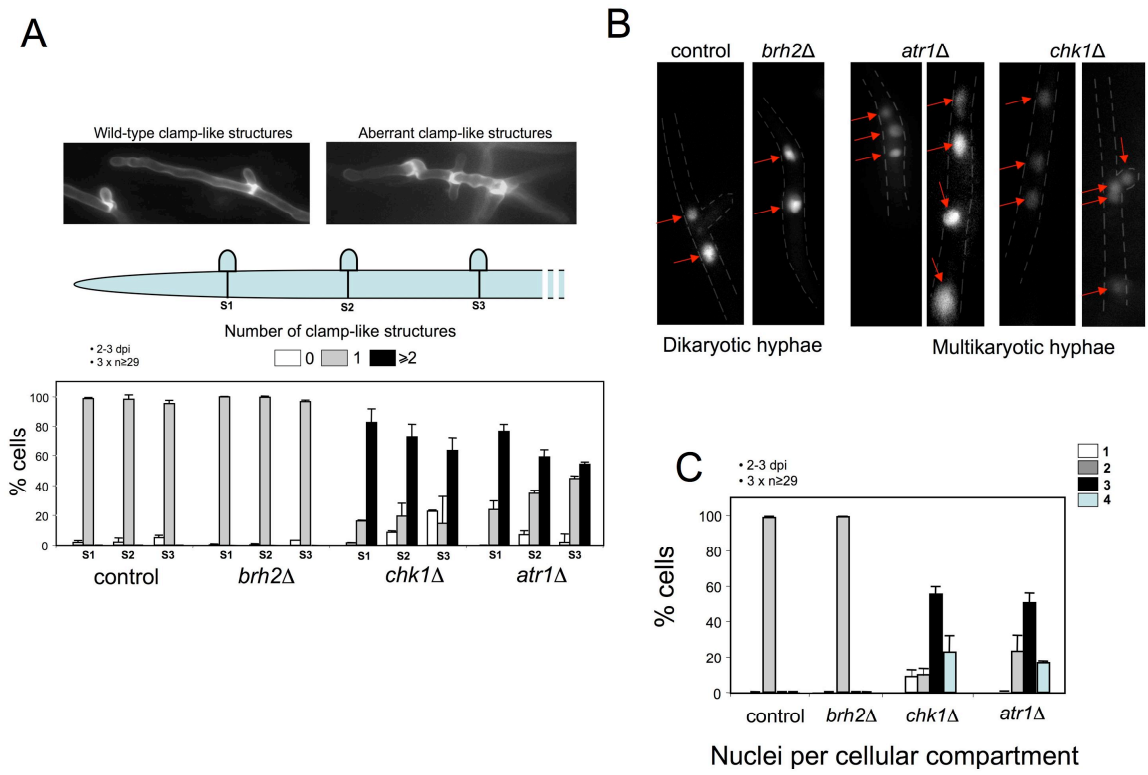

Figure 7. Atr1 and Chk1 are required for dikaryon maintenance *in planta*.
(A) Distribution of clamp-like structures in mutant cells. Infected plant tissue with the indicated strains was stained with WGA-AF488 and PI. Then individual hyphae were counted and sorted in function of the number of clamp-like structures observed at the three more apical septa (S1, S2 and S3). Control (wild-type) and *brh2*Δ filaments showed the expected distribution of one clamp-like structure per septum. Filaments defective in *chk1* or *atr1* showed a clear deviation of this pattern. Means and standard deviations are shown. Upper images exemplify typical wild-type (left) or mutant (right) hyphae.
(B) Examples of wild-type and the indicated mutant hyphae expressing a nuclear localized 3xGFP to detect nuclei. Wild-type hyphae contain two nuclei per cell as observed for *brh2*Δ. The *atr1*Δ and *chk1*Δ hyphae contain multiple nuclei per cell compartment. The distribution of the nuclei with respect to the clamp-like structures is given in the lateral illustrations.
(C) Quantification of the number of nuclei per cellular compartment in hyphae from infected plant tissue with the indicated strains. Means and standard deviations are shown.

de Sena-Tomas, Fig8

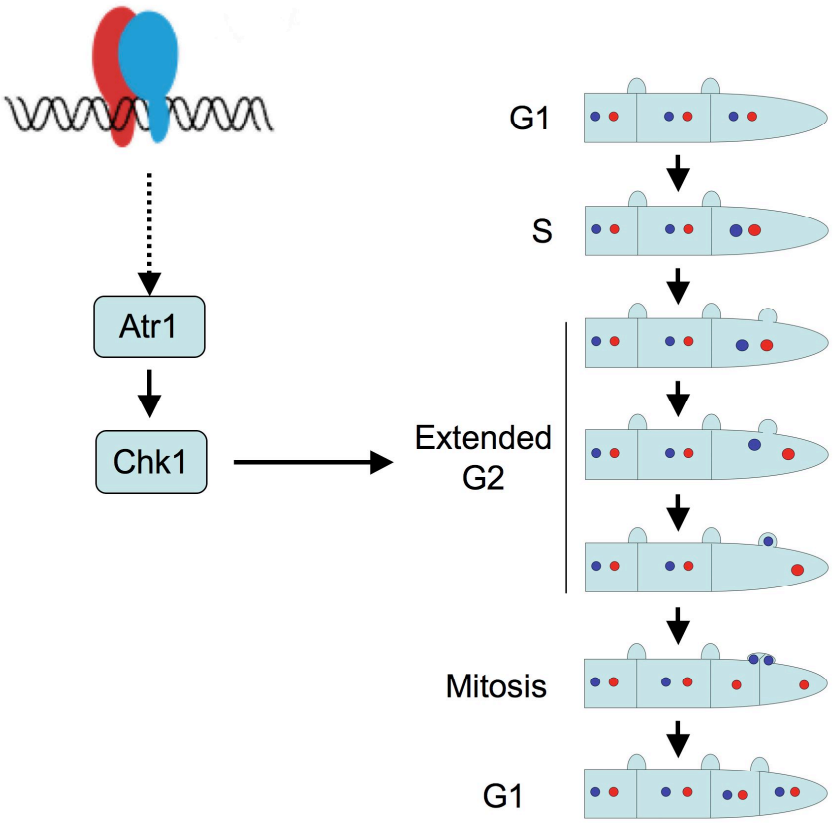

Figure 8. Working model of the role of Atr1-Chk1 axis during dikaryotic cell cycle. See text for description.